Chapter 3

Current interruption

In this chapter the current interrupt method, used for electrochemical characterisation of a PEM electrolyser, is discussed. Two equivalent electric circuits are developed by using two variants of the current interrupt method. The equivalent electric circuits consist of the Randles cell and the Randles-Warburg cell. With the Randles cell it is possible to model the activation and ohmic losses. The Randles-Warburg cell is used to model the activation, ohmic and concentration losses of the PEM electrolyser.

3.1 Introduction

In this chapter the working principle of the CI method is discussed. The current interrupt method is used to develop two equivalent electric circuits, namely the Randles cell and the Randles-Warburg cell. The EEC parameters of the Randles cell are calculated by means of the NVR method. The parameters of interest are the membrane resistance, the charge transfer resistance and the double layer capacitance.

Since it is not to possible to model the concentration losses with the Randles cell, the Randles-Warburg cell is also developed. The Randles-Warburg cell consists of the Randles cell parameters and the Warburg impedance. A depiction of the basic set-up is provided in Fig.3.1.

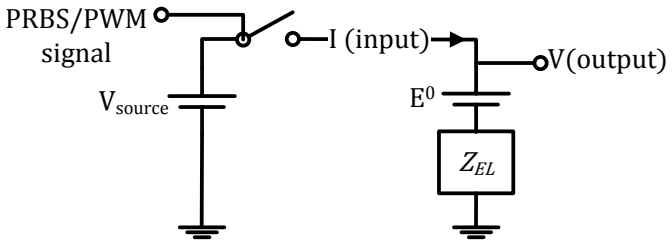

Figure 3.1: Basic setup for NVR and SI methods

It consists of a DC power source, the standard thermodynamic voltage, a PEM electrolyser and a switch. The switch is controlled by a switching signal, where the voltage and current waveforms are recorded. The recorded voltage and current data are used to develop equivalent electric circuits of the PEM electrolyser.

The thermodynamic voltage for the following chemical reaction

$$O_2 + 4H^+ + 4e^- \leftrightharpoons 2H_2O \tag{3.1}$$

is given by the standard electrode voltage [25], with E^0 = 1.229 V $\approx$ 1.23 V.

The voltage across the electrolyser can be expressed by the thermodynamic voltage, and the over-potentials caused by the activation, ohmic and concentration losses during cell operation. The expression for the electrolyser cell voltage is given by:

$$V_{cell} = E^0 + \eta_{act} + \eta_{ohm} + \eta_{con}, \tag{3.2}$$

where E^0 is the thermodynamic voltage, η_{act} is the activation over-potential, η_{ohm} is the ohmic over-potential and η_{con} is the concentration over-potential. In order to model only the equivalent electric circuit (Z_{EL}), it is necessary to subtract E^0 from the measured output voltage (V_{output}).

3.2 Natural voltage response method

The Randles cell is modelled by means of the NVR method. A depiction of the Randles cell is given in Fig. 3.2 with R_m the membrane resistance, R_{ct} the charge transfer resistance and C_{dl} the double layer capacitance.

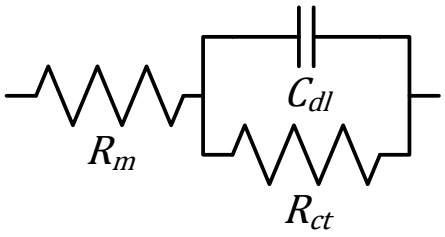

Figure 3.2: Equivalent electric circuit for NVR method: Randles cell

From Fig. 3.3 it is seen that the PEM electrolyser is operated at a specific voltage and current until steady state conditions are reached. At time t_0 the current is interrupted, by opening the switch, and a natural voltage response is observed.

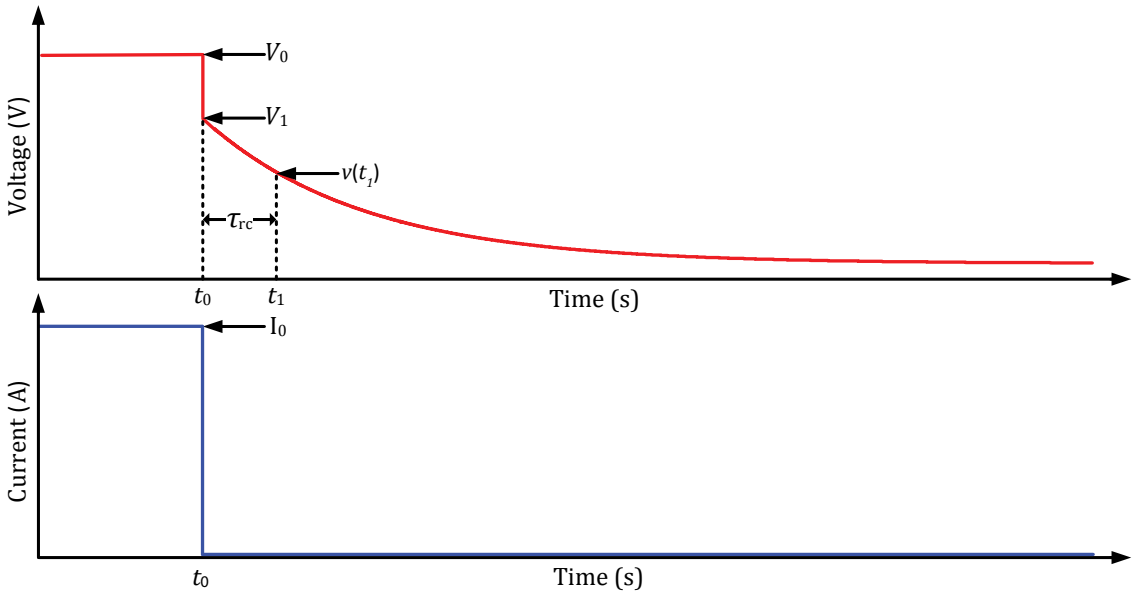

Figure 3.3: Typical current interrupt voltage and current transition

The voltage drop from V_0 to V_1 is a result of the ohmic losses within the PEM electrolyser, and the membrane resistance is calculated by

$$R_m = \frac{V_0 - V_1}{I_0}. \tag{3.3}$$

The voltage change from V_1 to V_2 is a result of the discharging of C_{dl} through R_{ct}, and the charge transfer resistance is calculated by

$$R_{ct} = \frac{V_1}{I_0}. \tag{3.4}$$

The voltage at t_1 is defined as [26]:

$$v(t_1) = (V_1)(e^{\frac{-t_1}{\tau_{rc}}}). \tag{3.5}$$

By solving for τ_{rc} in (3.5) the following is obtained:

$$\tau_{rc} = \frac{-t_1}{\ln(\frac{v(t_1)}{V_1})}. \tag{3.6}$$

The time constant (τ_{rc}) of a parallel RC circuit is defined as [26]:

$$\tau_{rc} = R_{ct}C_{dl}. \tag{3.7}$$

Once the value of the time constant is known, the double layer capacitance can be calculated by

$$C_{dl} = \frac{\tau_{rc}}{R_{ct}}. \tag{3.8}$$

3.3 Current switching method

The NVR method in combination with SI are used to obtain the EEC parameters of the Randles-Warburg cell. A depiction of the Randles-Warburg cell is given in Figure 3.4. The parameters of interest are the membrane resistance (R_m), charge transfer resistance (R_{ct}), double layer capacitance (C_{dl}) and the Warburg impedance (Z_{wbg}).

Figure 3.5 shows the typical waveforms which are generated during the current switching method. There are four stages during the CS method. During the first stage the NVR method is applied and the resulting voltage response is recorded. The parameter R_m is calculated using the NVR method described in section 3.2.

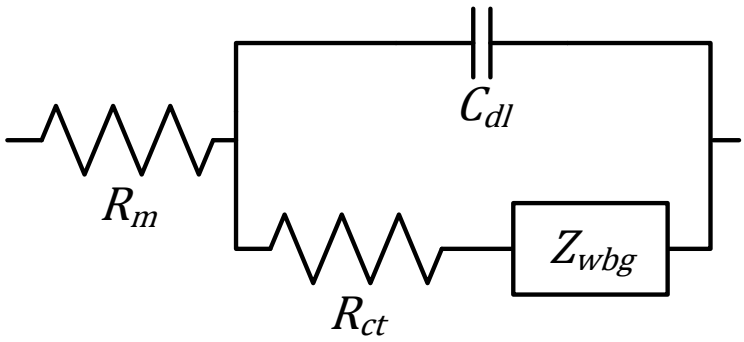

Figure 3.4: Equivalent electric circuit for CS method

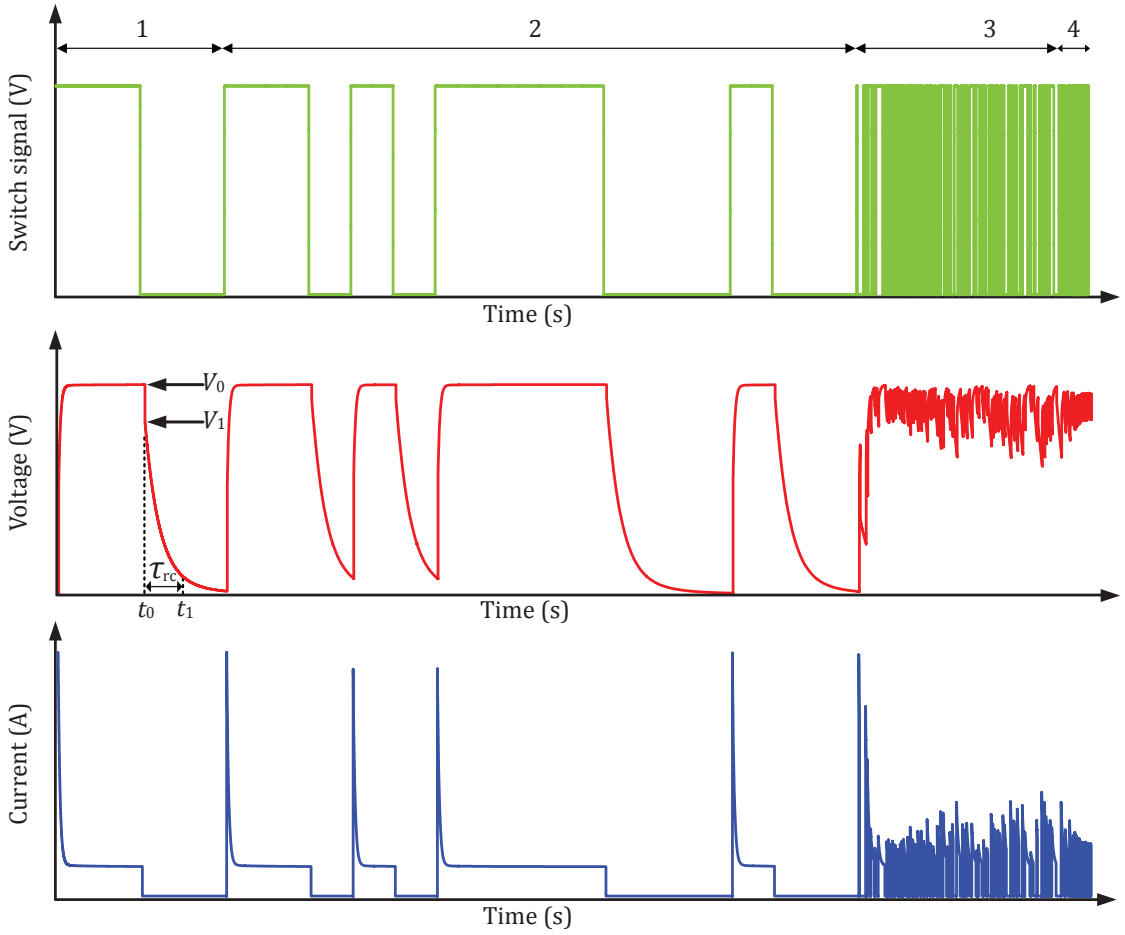

Figure 3.5: Input and output waveforms for CS method

During stages 2 to 4, three PRBS signals are applied to the switch and the resulting cell voltage and cell current signals are recorded. Since $Z(s) = V(s)/I(s)$, the current and voltage signals are used to obtain an impedance transfer function of the Randles-Warburg cell. System identification is used to generate a transfer function of the

Randles-Warburg cell. For the system identification process, the current signal is the input signal and the voltage signal is the output signal. Once the transfer function is generated, the parameters C_{dl}, R_{ct}, R_d, τ_d can be calculated.

3.3.1 PRBS design

The PRBS is selected as the perturbation signal, since it can be easily generated and applied as a switching signal. A PRBS signal is generated by shift register modulo 2 addition [5, 16]. The MLS pseudo random binary class is used to generate the PRBS signal. The number of binary levels, denoted N_{bl}, within a PRBS is given by $N_{bl} = 2^n - 1$, with n the number of flip flops within the shift register.

At first, the flip flops of the LFSR are arbitrarily initialised with a binary 0 or 1. This presents the ”pseudo random” characteristic of the PRBS signal. The binary condition of flip flop 8 is the first binary condition of the PRBS signal. After initialisation, each flip flop within the shift register is clocked once and shifts one bit to the right. Next the modulo 2 addition of the binary conditions in flip flop six and eight are calculated. The result is shifted into flip flop one and the process is repeated N_{bl} times.

A PRBS signal can be designed to excite a specific frequency range of interest. The frequency range of a PRBS is band limited and the available frequency range is only one third of the clock frequency [5]. Three PRBS signals are developed to excite a frequency range of interest, since it is impractical to design only one signal that contains all the frequencies [24]. When only one PRBS signal is developed the number of samples within the sequence becomes large.

The frequency at which the shift register is clocked is dependent on the maximum excitation frequency (f_{me}) and is given by [12]

$$f_{clk} = 2.5 f_{me}. \tag{3.9}$$

The clock period is obtained by taking the inverse of the clock frequency and is given

by

$$T_{clk} = \frac{1}{f_{clk}}. \tag{3.10}$$

The minimum and maximum frequencies are calculated by the following:

$$f_{min} = \frac{f_{clk}}{N_{bl}} \tag{3.11}$$

and

$$f_{max} = \frac{f_{clk}}{3}. \tag{3.12}$$

Three PRBS signals are used to excite a frequency range of $f_{min} = 0.267$ Hz to $f_{max} = 1.667$ kHz. The characteristics of the three PRBS signal are presented in Table 3.1.

Table 3.1: PRBS design characteristics

Parameter	PRBS 1	Unit	PRBS 2	Unit	PRBS 3	Unit
n	4	-	8	-	9	-
N_{bl}	15	-	255	-	511	-
f_{me}	1.6	Hz	80	Hz	2	kHz
f_{clk}	4	Hz	200	Hz	5	kHz
f_{min}	0.267	Hz	0.784	Hz	9.785	Hz
f_{max}	1.333	Hz	66.67	Hz	1.667	kHz
T_{clk}	250	ms	5	ms	200	μs
T_{per}	3.75	s	1.275	s	0.1022	s

In Figure 3.6 (a) is a depiction of a 4-bit LFSR. The 4-bit LFSR is initialised with 1011 and the generated PRBS waveform is presented in Figure 3.6 (b). The ACF and the PSD of the first PRBS signal is shown in Figure 3.6 (c) and Figure 3.6 (d), respectively. In Figure 3.7 (a) is a depiction of a 8-bit LFSR is given. The 8-bit LFSR is initialised with 00000001 and the generated PRBS waveform is presented in Figure 3.7 (b). The ACF and the PSD of the second PRBS signal is depicted in Figure 3.7 (c) and Figure 3.7 (d), respectively. Figure 3.8 (a) portrays a 9-bit LFSR. The 9-bit LFSR is initialised with 000000001 and the generated PRBS waveform is presented in Figure 3.8 (b). The ACF and the PSD of the third PRBS signal is portrayed in Figure 3.8 (c) and Figure 3.8 (d), respectively.

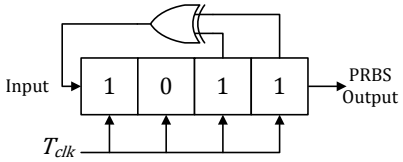

(a)

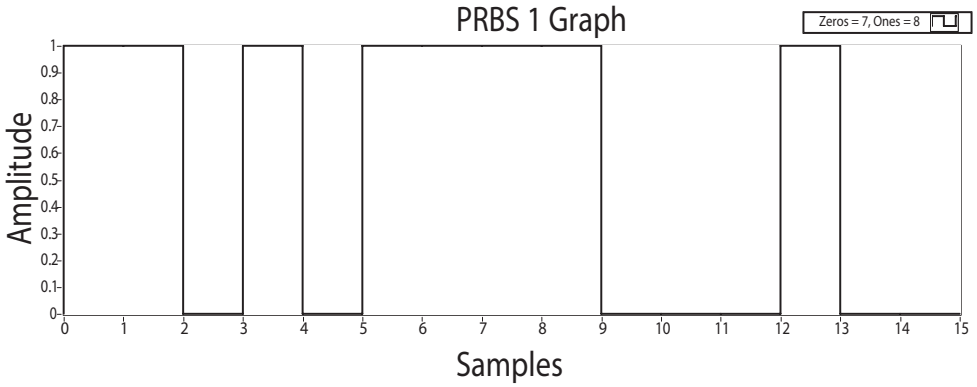

(b)

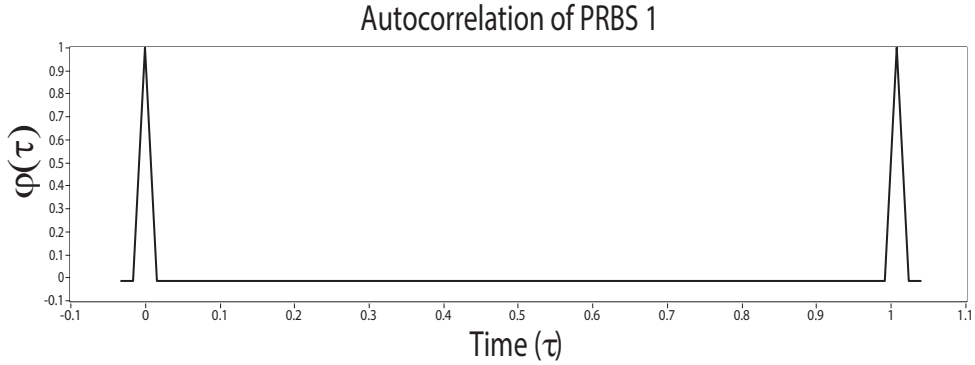

(c)

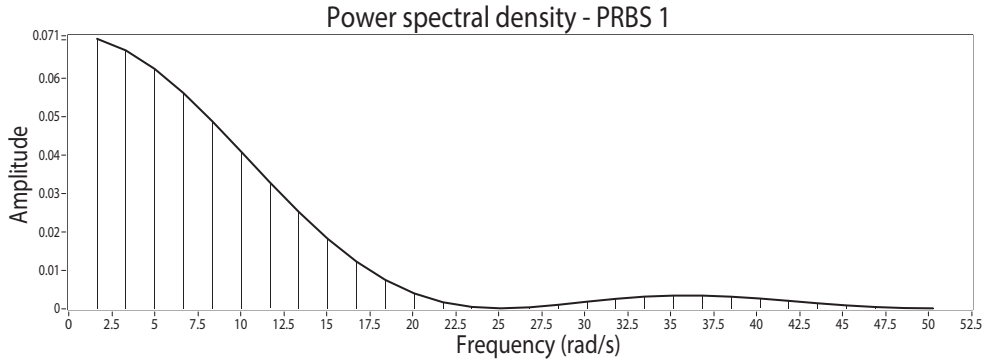

(d)

Figure 3.6: PRBS 1: (a) 4 bit LFSR (b) Switching signal (c) ACF graph (d) PSD graph

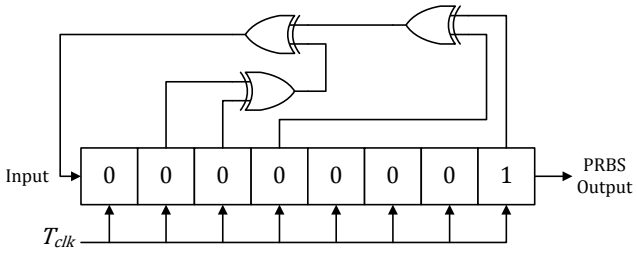

(a)

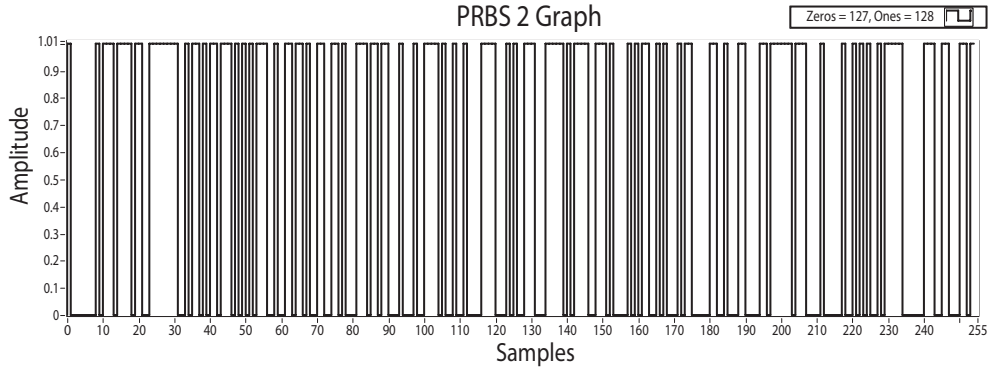

(b)

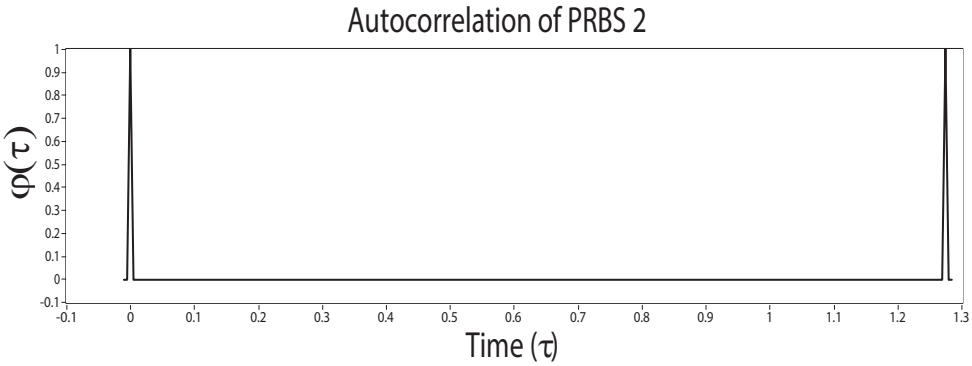

(c)

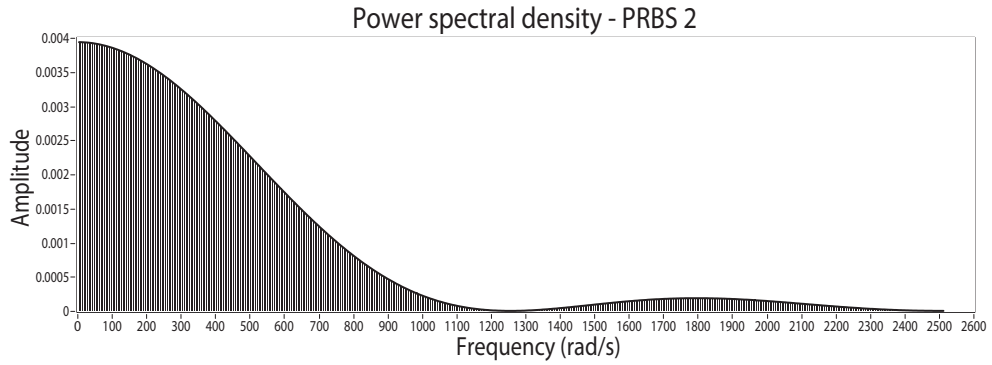

(d)

Figure 3.7: PRBS 2: (a) 8 bit LFSR (b) Switching signal (c) ACF graph (d) PSD graph

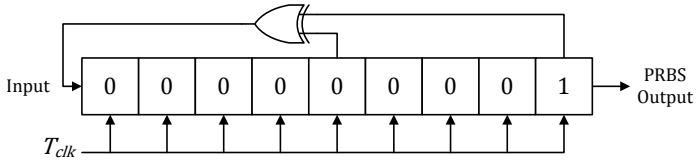

(a)

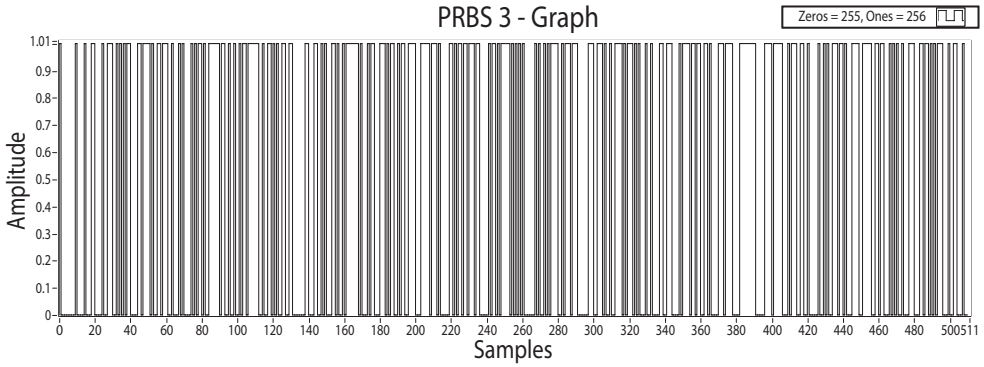

(b)

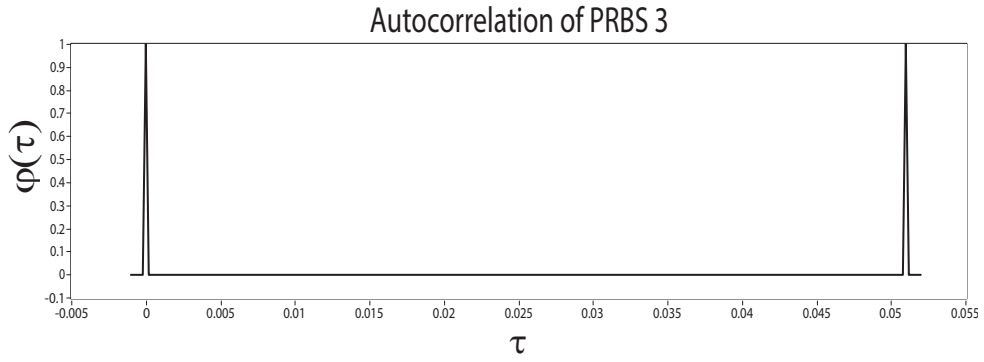

(c)

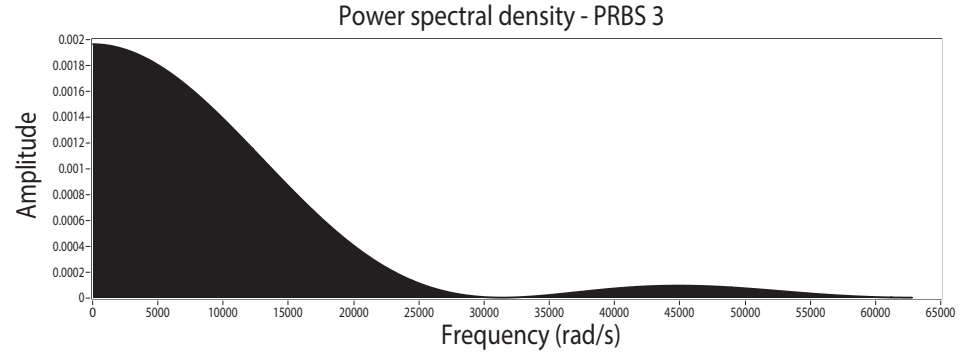

(d)

Figure 3.8: PRBS 3: (a) 9 bit LFSR (b) Switching signal (c) ACF graph (d) PSD graph

3.3.2 Warburg modelling

The Warburg impedance relates to the concentration losses within the PEM electrolyser, and is most significant at low frequencies and high current densities [27]. The analytical expression for the Warburg impedance is given in (3.13):

$$Z_{w\_an}(s) = R_d \left(\frac{\tanh \sqrt{s\tau_d}}{\sqrt{s\tau_d}} \right) \tag{3.13}$$

with R_d is the diffusion resistance and τ_d is the diffusion time constant [27].

The Warburg impedance given in (3.13) can be approximated by means of the impedance transfer function of a RC electric circuit [23].

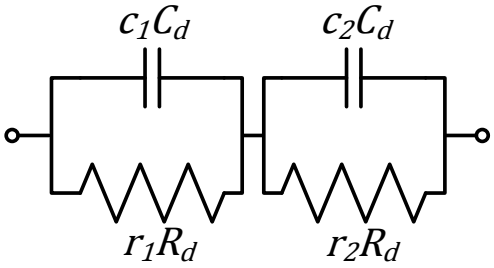

Figure 3.9: Warburg impedance equivalent electric circuit

A depiction of the approximated Warburg impedance, denoted Z_{wbg}, is given in Fig. 3.9. It consists of two electrical components R_d and C_d, with r_1, c_1, r_2 and c_2 the dimensionless Warburg coefficients.

$$Z_{wbg}(s) = R_d \left(\frac{r_1}{(r_1 c_1 \tau_d)s + 1} + \frac{r_2}{(r_2 c_2 \tau_d)s + 1} \right) \tag{3.14}$$

with $\tau_d = R_d C_d$.

From (3.13) and (3.14) it is seen that,

$$\left(\frac{\tanh \sqrt{s\tau_d}}{\sqrt{s\tau_d}} \right) \approx \left(\frac{r_1}{(r_1 c_1 \tau_d)s + 1} + \frac{r_2}{(r_2 c_2 \tau_d)s + 1} \right) \tag{3.15}$$

The Warburg coefficients r_1, c_1, r_2 and c_2 are estimated by fitting the right part of (3.15) to the left, and are calculated by means of a Levenberg-Marquardt algorithm. The coefficients are estimated for equally spaced values of frequency and the diffusion time constant τ_d. The Warburg coefficients were estimated for values of (s) from 0.002π rad/s to 500π rad/s, and (τ_d) from 1 ms to 10 s. Values for (s) and (τ_d) are selected which represents the practical system.

The Warburg plot, consisting of a comparison between the analytical and fitted data, is depicted in Figure 3.11.

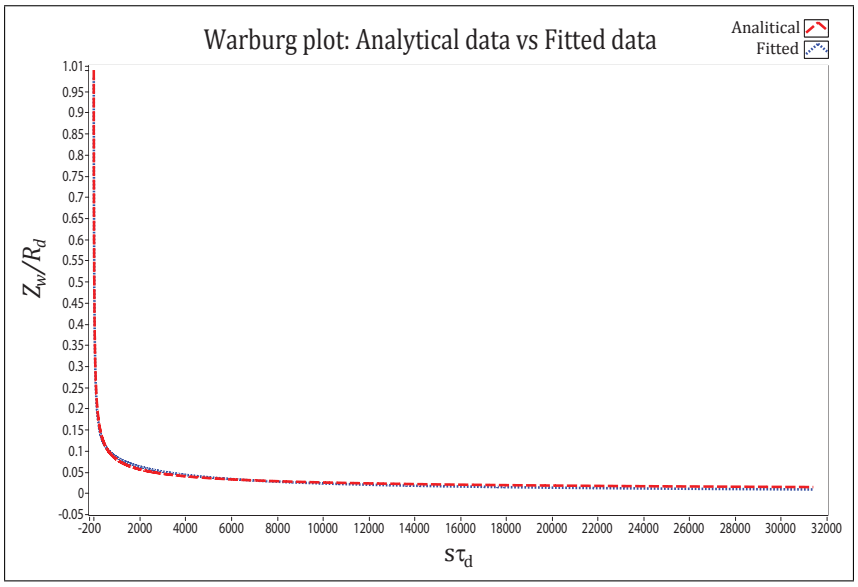

Figure 3.10: Warburg plot: Analytical data plotted vs fitted data

The Warburg Nyquist plot, consisting of a comparison between the analytical and fitted data, is depicted in Figure 3.11. The Nyquist plot illustrates the impedance of the Warburg impedance in the complex domain.

The Warburg coefficients are accurately calculated with a Mean Squared Error (MSE) of 2.586e-6. The calculated Warburg coefficient values are presented in Table 3.2.

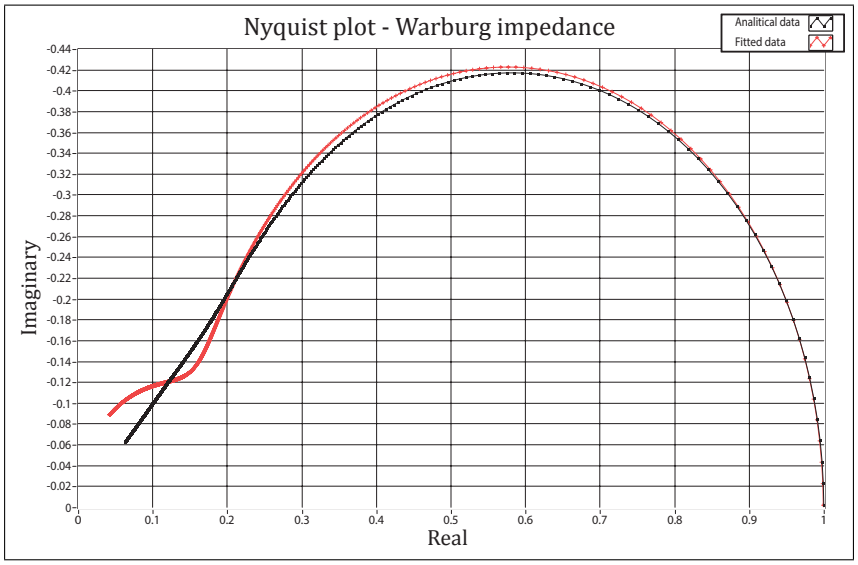

Figure 3.11: Nyquist plot: Analytical data plotted vs fitted data

Table 3.2: Calculated Warburg coefficients

Warburg coefficient	Value
r_1	0.097
c_1	0.027
r_2	0.888
c_2	0.360

3.3.3 Equivalent electric circuit transfer function

The EEC of the Randles-Warburg cell is given in Figure 3.12.

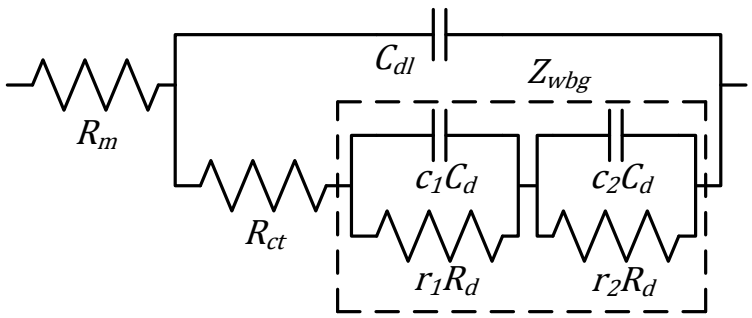

Figure 3.12: Complete Randles-Warburg cell

The transfer function of the Randles-Warburg cell is given in (3.16).

$$Z_{RW} = \frac{as^3 + bs^2 + cs + d}{es^3 + fs^2 + gs + 1} \tag{3.16}$$

with,

$$a = c_1 c_2 r_1 r_2 C_{dl} R_{ct} R_m \tau_d^2 \tag{3.17}$$

$$b = c_1 c_2 r_1 r_2 (R_{ct}\tau_d^2 + R_m \tau_d^2) + C_{dl} R_{ct} R_m \tau_d (c_1 r_1 + c_2 r_2) + C_{dl} R_d R_m \tau_d (c_1 r_1 r_2 + c_2 r_1 r_2) \tag{3.18}$$

$$c = C_{dl} R_{ct} R_m + C_{dl} R_d R_m (r_1 + r_2) + R_{ct} \tau_d (c_1 r_1 + c_2 r_2) + R_m \tau_d (c_1 r_1 + c_2 r_2) + R_d \tau_d (c_1 r_1 r_2 + c_2 r_1 r_2) \tag{3.19}$$

$$d = R_{ct} + R_m + R_d (r_1 + r_2) \tag{3.20}$$

$$e = c_1 c_2 r_1 r_2 C_{dl} R_{ct} \tau_d^2 \tag{3.21}$$

$$f = C_{dl} R_{ct} \tau_d (c_1 r_1 + c_2 r_2) + C_{dl} R_d \tau_d (c_1 r_1 r_2 + c_2 r_1 r_2) + c_1 c_2 r_1 r_2 \tau_d^2 \tag{3.22}$$

$$g = C_{dl} R_{ct} + C_{dl} R_d (r_1 + r_2) + r_1 \tau_d (c_1 + c_2). \tag{3.23}$$

The parameters (R_m, R_{ct}, C_{dl}, R_d and τ_d) are calculated by generating real values for the transfer function coefficients and solving the system of simultaneous equations. Since there are five unknowns to solve, only five of the simultaneous equations are used to calculate the parameters. Equations (3.17) and (3.21) does not influence the solution, therefore the subset of simultaneous equations consist of equations (3.18), (3.19), (3.20), (3.22) and (3.23). This reduces the model complexity and the computation time. Once R_m is calculated, using the NVR method, it can be substituted into the subset of simultaneous equations. This further reduces the complexity of calculating the remaining parameters.

3.4 Conclusion

The CI method, used for solving the parameters of the Randles cell and the Randles-Warburg cell, is proposed. A thorough and detailed discussion of the NVR method and the CS method is presented. Since the method is developed it can be implemented by means of simulation. The simulation provides a platform for model testing, method verification and validation.